The Astrophysical Journal Letters, 768:L28 (5pp), 2013 May 10 doi:10.1088/2041-8205/768/2/L28

FOSSIL EVIDENCE FOR THE TWO-PHASE FORMATION OF ELLIPTICAL GALAXIES

Song Huang (黄崧)[1,2,3], Luis C. Ho[2], Chien Y. Peng[4], Zhao-Yu Li (李兆聿)[5], and Aaron J. Barth[6]
[1] School of Astronomy and Space Science, Nanjing University, Nanjing 210093, China
[2] The Observatories of the Carnegie Institution for Science, 813 Santa Barbara Street, Pasadena, CA 91101, USA
[3] Key Laboratory of Modern Astronomy and Astrophysics, Nanjing University, Nanjing 210093, China
[4] Giant Magellan Telescope Organization, 251 South Lake Avenue, Suite 300, Pasadena, CA 91101, USA
[5] Key Laboratory for Research in Galaxies and Cosmology, Shanghai Astronomical Observatory, Chinese Academy of Sciences, 80 Nandan Road, Shanghai 200030, China
[6] Department of Physics and Astronomy, 4129 Frederick Reines Hall, University of California, Irvine, CA 92697-4575, USA
Received 2012 December 13; accepted 2013 April 5; published 2013 April 24

ABSTRACT

Massive early-type galaxies (ETGs) have undergone dramatic structural evolution over the last 10 Gyr. A companion paper shows that nearby elliptical galaxies with $M_* \geqslant 1.3 \times 10^{11} M_\odot$ generically contain three photometric subcomponents: a compact inner component with effective radius $R_e \lesssim 1$ kpc, an intermediate-scale middle component with $R_e \approx 2.5$ kpc, and an extended outer envelope with $R_e \approx 10$ kpc. Here we attempt to relate these substructures with the properties of ETGs observed at higher redshifts. We find that a hypothetical structure formed from combining the inner and middle components of local ellipticals follows a strikingly tight stellar mass–size relation, one that resembles the distribution of ETGs at $z \approx 1$. Outside of the central kpc, the median stellar mass surface density profiles of this composite structure agree closest with those of massive galaxies that have similar cumulative number density at $1.5 < z < 2.0$ within the uncertainty. We propose that the central substructures in nearby ellipticals are the evolutionary descendants of the "red nuggets" formed under highly dissipative ("wet") conditions at high redshifts, as envisioned in the initial stages of the two-phase formation scenario recently advocated for massive galaxies. Subsequent accretion, plausibly through dissipationless ("dry") minor mergers, builds the outer regions of the galaxy identified as the outer envelope in our decomposition. The large scatter exhibited by this component on the stellar mass–size plane testifies to the stochastic nature of the accretion events.

Key words: galaxies: evolution – galaxies: photometry – galaxies: structure

Online-only material: color figures

1. INTRODUCTION

Recent observations have established that high-redshift early-type galaxies (ETGs) are more compact (Daddi et al. 2005; Trujillo et al. 2006; Damjanov et al. 2011) and have higher stellar velocity dispersions (Cappellari et al. 2009; Onodera et al. 2012) than nearby ETGs of the same stellar mass. Since $z \approx 2.5$, "red nuggets" on average have doubled in stellar mass and increased their size by a factor of 3–4 (Buitrago et al. 2008; van Dokkum et al. 2010; Papovich et al. 2012; Szomoru et al. 2012). Some appear to have a disk-like morphology (van der Wel et al. 2011) and are always bluer in the outskirts (Gargiulo et al. 2012). The accumulated evidence suggests that massive ETGs build up inside-out through non-dissipational processes (Bezanson et al. 2009; van Dokkum et al. 2010).

These developments severely challenge classical models of elliptical (E) galaxy formation such as monolithic collapse (Larson 1975) and binary major mergers (Toomre & Toomre 1972; Negroponte & White 1983). Instead, the current evidence favors a "two-phase" scenario (Oser et al. 2010; Johansson et al. 2012). Intense dissipational processes such as cold accretion (Dekel et al. 2009) or gas-rich mergers rapidly build up an initially compact progenitor. After star formation is quenched, a second phase of slower, more protracted evolution is dominated by non-dissipational processes such as dry, minor mergers. For such a scenario to work, the rate of minor mergers (Bluck et al. 2012; Newman et al. 2012) has to be consistent with the prevalence of faint companion galaxies at high redshifts. Perhaps other mechanisms may also be important, such as major merger (Saracco et al. 2011; Bernardi et al. 2011; Prieto et al. 2013) or active galactic-nucleus-induced expansion (Fan et al. 2008). Given that large uncertainties remain in identifying the relevant physics and quantifying their detailed balance, a key sanity check is to see whether one can separate out the fossil bodies of compact $z > 1.5$ galaxies at the core of nearby galaxies. This separation is successful only when several clear and solid predictions, especially the similarity between the core components and the high-z compact progenitors in mass versus size relation and detailed mass profile, are met. These stringent predictions are the basis of this study to verify or falsify. We assume a ΛCDM cosmology with $\Omega_m = 0.27$, $\Omega_\Lambda = 0.73$, and $H_0 = 73$ km s^{-1} Mpc^{-1}.

2. OBSERVATIONAL MATERIAL

This work uses the three-component models of nearby Es from the Carnegie–Irvine Galaxy Survey (CGS; Ho et al. 2011), a systematic study of 605 bright ($B_T < 12.9$ mag) southern ($\delta < 0^\circ$) galaxies. The currently completed photometric part of CGS includes *BVRI* images obtained using the 100 inch du Pont Telescope at Las Campanas Observatory, using a $8\farcm9 \times 8\farcm9$ detector with a pixel scale of $0\farcs259$, under $\sim 1''$ seeing conditions. More details on the observations and data reductions can be found in Ho et al. (2011) and Li et al. (2011).

Huang et al. (2013) apply GALFIT (Peng et al. 2010) to perform a detailed two-dimensional analysis of the *V*-band images of 94 CGS Es. Their decomposition reveals that,

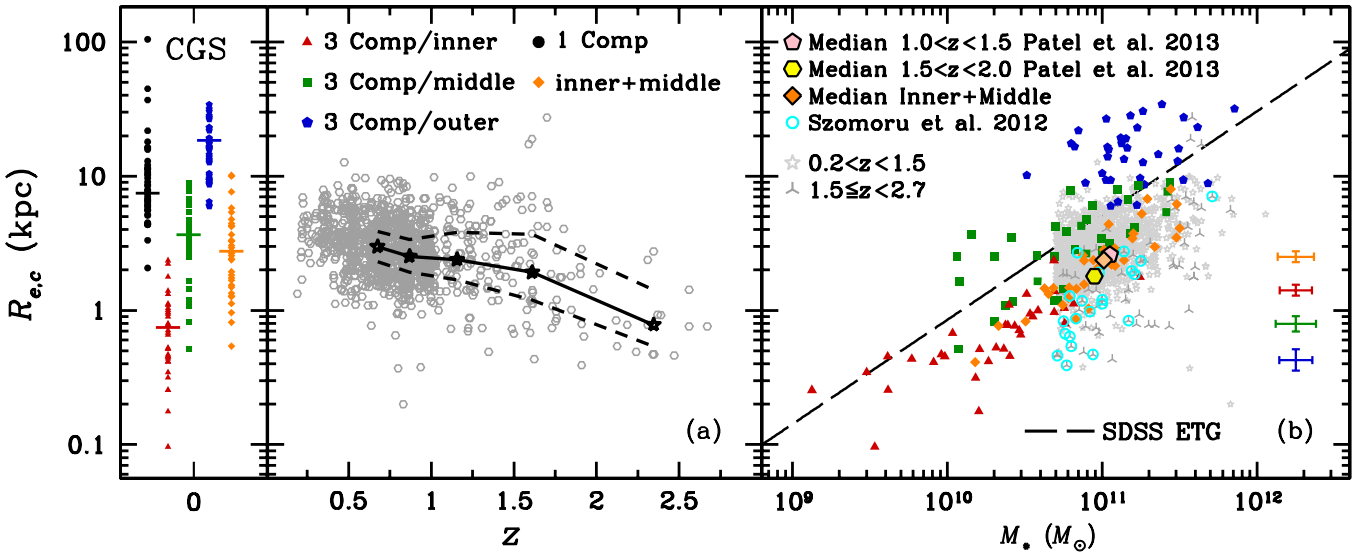

Figure 1. Redshift evolution of size and its relation with stellar mass for nearby Es and high-z ETGs. The left side of panel (a) summarizes the size distributions of single-component models (black circles) and the inner (red triangles), middle (green squares), and outer (blue pentagons) components of the three-component models of CGS Es. The median of each distribution is marked by a horizontal bar. The right side illustrates the redshift evolution for high-z ETGs with $M_* \geqslant 10^{10.7}\ M_\odot$ (gray open circles). The solid and dashed lines give the running median and its associated first and third quartile through five redshift bins ($0.50 \leqslant z < 0.75$, $0.75 \leqslant z < 1.0$, $1.0 \leqslant z < 1.4$, $1.4 \leqslant z < 2.0$, and $2.0 \leqslant z \leqslant 2.7$). Panel (b) shows the mass–size relation for high-z ETGs, separated into those with $z < 1.5$ (gray stars) and $z \geqslant 1.5$ (gray skeletal triangles). The 21 massive ETGs at $1.5 < z < 2.5$ from Szomoru et al. (2012) are marked with cyan circles. Each of the three subcomponents of the CGS sample is plotted separately, as well as for the inner + middle components combined (orange diamonds). Also highlighted are the median properties for the inner + middle components of the CGS Es and for the massive galaxies at $1.0 < z < 1.5$ and $1.5 < z < 2.0$ selected by their cumulative number density from Patel et al. (2013). Typical error bars for the subcomponents are shown on the lower-right corner. The best-fit relation of Guo et al. (2009) for local SDSS ETGs is plotted with a dashed line. For consistency with the high-z measurements, the effective radii used here are the so-called mean, or circularized, radii, such that $R_{e,c} = R_e \sqrt{b/a}$, where b/a is the axis ratio.

(A color version of this figure is available in the online journal.)

contrary to popular perception, the global light distribution of most nearby Es have more complicated structures than can be described by a single Sérsic (1968) profile. Instead, 70 out of the 94 Es can be fit with 3 distinct subcomponents: (1) an inner, compact center with effective radius $R_e \lesssim 1$ kpc comprising a small fraction of the light ($f \approx 0.1$–0.15); (2) an intermediate-scale, middle structure with $R_e \approx 2.5$ kpc and $f \approx 0.2$–0.25; and (3) an outer, dominant, extended, moderately flattened envelope with $R_e \approx 10$ kpc and $f \approx 0.6$.

The image decomposition was performed without ascribing any physical significance to the substructure. Nevertheless, the fact that the individual subcomponents define distinct sequences on the size–luminosity plane, and that three-component fits often seemed naturally preferred, hint at the possibility that the subcomponents reflect underlying physical reality. Here we compare some key properties of the three-component models of local Es with observations of high-z ETGs to shed new light on the structural evolution of massive galaxies.

For this purpose, we compiled stellar masses and effective radii for 1323 high-z ETGs with stellar masses $M_* \geqslant 10^{10.7}\ M_\odot$ as follows: 352 ($0.2 < z < 2.7$) from Damjanov et al. (2011); 910 ($0.2 < z < 1.2$) from COSMOS (Scoville et al. 2007; using morphological classification from Scarlata et al. 2007 and Tasca et al. 2009); 32 ($1.5 < z < 3$, choosing Sérsic indices $n > 2$) from the GOODS-NICMOS survey (Conselice et al. 2011); 8 ($z \approx 1.6$, $n > 2$) from Papovich et al. (2012); and 21 ($1.5 < z < 2.5$) from CANDELS (Grogin et al. 2011), as analyzed by Szomoru et al. (2012). Although the sample is in many respects heterogeneous (in terms of observed bandpass, selection criteria, modeling method), the general trends we explore in this Letter should not be strongly affected, as demonstrated by Damjanov et al. (2011).

3. LINKING NEARBY AND HIGH-z EARLY-TYPE GALAXIES

Figure 1(a) illustrates the redshift evolution of galaxy size for massive ETGs. Although the scatter is substantial, the size increase with decreasing z is confirmed (e.g., Damjanov et al. 2011; Cimatti et al. 2012). The median circularized effective radius increases from 0.8 kpc at $2.0 \leqslant z \leqslant 2.7$, to $R_{e,c} \approx 1.9$ kpc at $1.4 \leqslant z < 2.0$, to $R_{e,c} \approx 3$ kpc at $0.50 \leqslant z < 0.75$. By $z = 0$, Es have reached a median $R_{e,c} = 7.5$ kpc according to the single-component fits applied to the subsample of 35 massive CGS Es that satisfy $M_* \gtrsim 10^{11}\ M_\odot$ (solid black points). The CGS mass cut roughly corresponds to twice the mass limit of the high-z sample.

How are the subcomponents of nearby Es related to the high-z systems? Judging by the distribution of sizes for the subcomponents shown on the left side of Figure 1(a), the typical effective radius of the inner component (median $R_{e,c} = 0.9$ kpc) does overlap substantially with that of high-z red nuggets; however, their stellar masses, only ~10%–15% of the total, are about a factor of 3–5 lower than the high-z systems (Figure 1(b)). The middle component, with median $R_{e,c} = 3.7$ kpc, matches well the sizes and masses of ETGs at $z \approx 0.5$, but they are still on average more extended than those at $z > 1.0$. On the other hand, with median $R_{e,c} = 17.5$ kpc, the outer component of local Es is clearly larger than the globally averaged size of most ETGs at any redshift.

The mass–size relation offers another vantage point. As described in Huang et al. (2013), single-component fits to the CGS Es produce sizes that follow well the mass–size relation of local ETGs selected from the Sloan Digital Sky Survey (SDSS; Guo et al. 2009; dashed line in Figure 1(b)). As expected, high-z

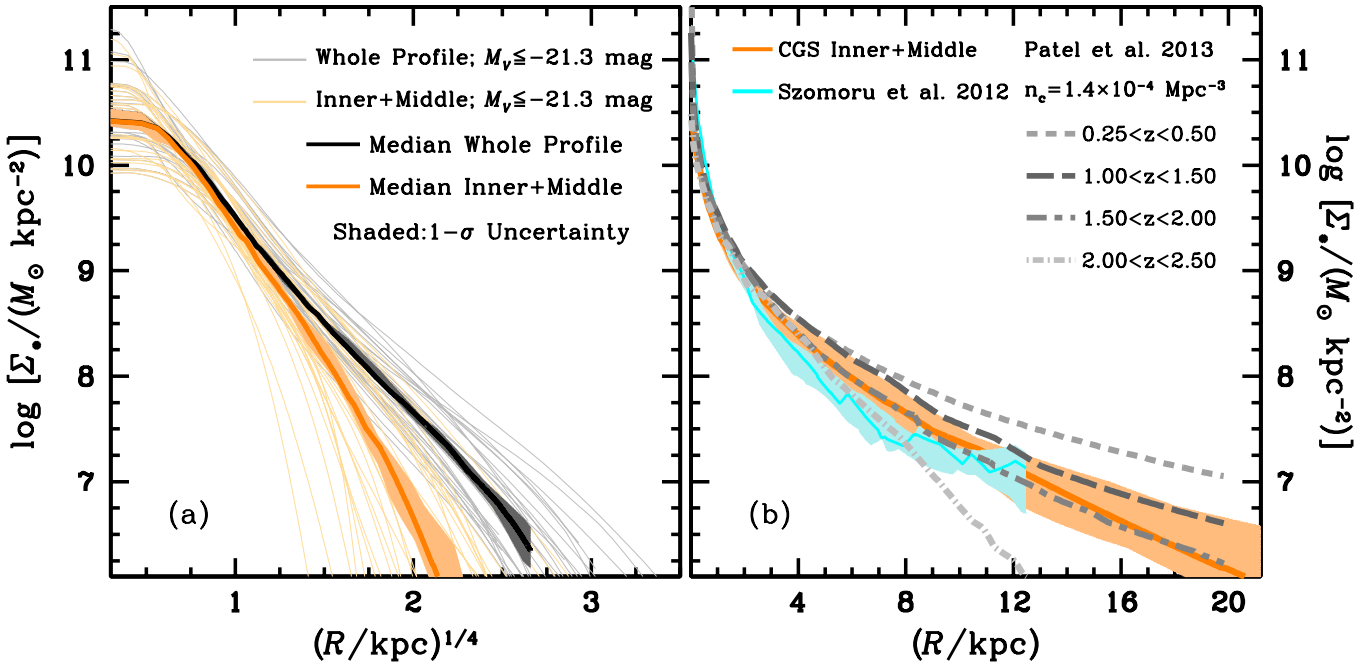

Figure 2. (a) Mass surface density profiles for CGS Es with $M_V \leqslant -21.3$ mag. The individual profiles for the entire galaxy and for the combined inner + middle components are plotted in light gray and orange, respectively; their corresponding median profiles are plotted as darker solid lines, with the shaded region denoting the associated 1σ uncertainty range of the median value (determined from bootstrap resampling). (b) Comparison of the median profile of the inner + middle components for CGS Es (orange solid line; shaded region 1σ uncertainty) with the median profiles for massive galaxies at different redshift bins selected by their cumulative number density ($n_c = 1.4 \times 10^{-4}$ Mpc^{-3}; Patel et al. 2013). The median profile (and associated uncertainty) for the 21 massive ETGs at $1.5 < z < 2.5$ from Szomoru et al. (2012) is also shown. Note that the radial scale is plotted as $R^{1/4}$ in (a) but as linear in R in (b) to emphasize the outer regions.

(A color version of this figure is available in the online journal.)

ETGs, especially those with $z \geqslant 1.5$, fall systematically below the local relation. At fixed stellar mass, high-z systems are a factor ∼4–5 more compact than their $z = 0$ counterparts. While the inner component of the CGS galaxies is generally not massive enough to directly map onto high-z objects, the middle component can be viewed as a slightly modified version of the compact quiescent galaxies. The mass–size relation for the middle component runs roughly parallel to, but is offset slightly below, that of local ETGs. It lies approximately in between the locus of high-z and low-z points. In dramatic contrast with the inner and middle components, the outer envelope displays significantly larger scatter on the R_e–M_* plane. While some of the scatter undoubtedly arises from measurement uncertainty, which, as indicated at the bottom-right corner of Figure 1(b), is considerable for extended, low-surface brightness features, we believe that most of the scatter is intrinsic.

As discussed in Huang et al. (2013), the central core may have been reshaped more recently (Hopkins et al. 2009a, 2009b, 2009c) than the overall compact stellar body of interest, thus requiring a separate component to model well in order to sensitively extract the lower lying outer component. Regardless of the exact process that shaped the small central structure, it is a small perturbation to the overall structure of interest, hence we group the innermost two components (designated henceforth as "inner + middle") into a single entity. To measure the overall size, mass, and profile of the composite, we generated model images from best-fit parameters that summed the innermost subcomponents, accounting for the point-spread function (PSF). Then, we fit a single-component model to extract the effective radius of this composite structure. As the inner component has higher density than the middle one, we intuitively expect the effective radius of the combined structure to be smaller than that of the middle component alone. This is indeed the case, as Figure 1(b) shows. Surprisingly, the composite inner + middle structure (orange diamonds) not only forms a very tight mass–size relation with a slope similar to that of Guo et al. (2009) for SDSS ETGs, but it also lies on top of the distribution of points for most high-z ETGs, especially those with $z < 1.5$.

As advocated by van Dokkum et al. (2010), galaxies selected at constant cumulative number density provide a more physical connection between progenitors and descendants than those selected above a constant stellar mass. We therefore compare our observations with the sample of Patel et al. (2013), which is selected at a cumulative number density ($n_c = 1.4 \times 10^{-4}$ Mpc^{-3}) that corresponds to massive ETGs ($M_* \approx 10^{11.2}\,M_\odot$) similar to the CGS sources at $z \approx 0$. Figure 1(b) shows that the median M_* and R_e of our inner + middle components agree quite well with the properties of galaxies at $1.0 < z < 1.5$ from Patel et al. (2013). Apart from global quantities such as mass and effective radius, the surface density profiles themselves provide a more direct comparison of the structural connection between high-z ETGs and local Es. For this purpose, we convert the surface brightness profiles of the inner + middle components, after removing the PSF smearing, into stellar mass density profiles using the mass-to-light ratio adopted in Huang et al. (2013). Their median profile is shown in Figure 2(a), and in Figure 2(b) we compare it to the median profiles of the cumulative number density-selected galaxies in different redshift bins from Patel et al. (2013). The median profile of the inner + middle components of local Es matches quite closely the profiles of massive galaxies at $1.5 < z < 2.0$ over most of their radial extent. Unlike the median M_* and R_e, the median profile of $1.0 < z < 1.5$ massive galaxies is only marginally close to the profile of inner + middle component. This seemingly difference relates to the higher density of high-z objects at $R < 1.0$ kpc. It

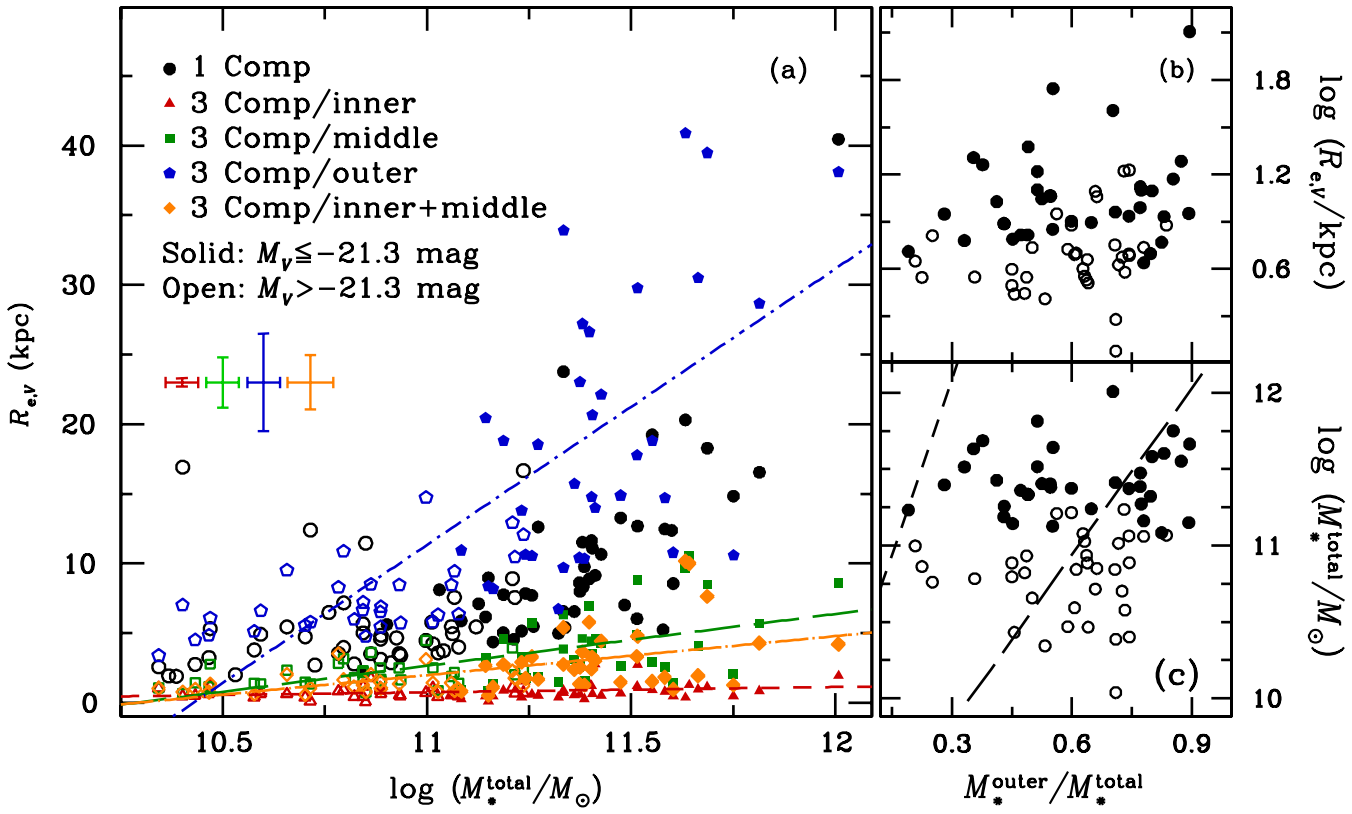

Figure 3. (a) Correlations between R_e of different components and total stellar mass M_*^{total}. The symbols are the same as in Figure 1(a); the linear correlations from least-squares fitting are shown using the same color scheme as the points. The two right panels show the dependence between the mass fraction of the outer component and R_e from single-component models (b) and M_*^{total} (c). The two lines in panel (c) represent the relation between accreted mass fraction (which we approximate with M_*^{outer}/M_*^{total}) and M_*^{total} from the simulations of Oser et al. (2010; long dashed line) and Lackner et al. (2012; short dashed line). Note that for the purposes of this comparison we make use of the full sample 70 CGS Es with robust multi-component fits, not just the high-luminosity subsample.

(A color version of this figure is available in the online journal.)

is confirmed in the median density profile of the massive ETGs at $1.5 < z < 2.5$ from Szomoru et al. (2012), which show even higher central densities than the sample from Patel et al. at comparable redshifts. This apparent discrepancy may be due to different selection criteria employed in the two studies.

The two-phase formation scenario of ETGs (Oser et al. 2010; Johansson et al. 2012) offers an appealing framework to interpret the above trends and to connect the distant and local populations of massive galaxies. Dissipative processes ("in situ" star formation, in the language of Oser et al. 2010) connected with early gas-rich events naturally lead to high central densities. We suggest that the central, more compact structures of nearby Es—namely, the "inner" or "middle" components, possibly both—are the natural outcomes of this initial, dissipative phase. We propose that they are the direct remnants of the high-z massive quiescent galaxies. The combined luminosity (mass) fraction of the inner + middle components, $f \approx 0.3$–0.4, is roughly comparable to the factor of $\sim$2 increase necessary to grow the high-z objects, if they are the progenitors of local Es. Their overall physical scales are also consistent with their originally compact nature. In detail, the current evidence suggests that the high-z objects tend to have somewhat higher central densities than their local remnants. This is an important constraint that future theoretical models should try to reproduce.

We equate the extended outer envelope with material accreted through dissipationless minor mergers ("ex situ" stars; Oser et al. 2010). The large intrinsic scatter on the R_e–M_* plane is likely related to the stochastic nature by which the outer envelope is expected to have accumulated. The minor merger hypothesis has previously been questioned on the basis of the apparently small observed scatter of the mass–size relation of nearby Es (Nipoti et al. 2012). For those two observations to be consistent, dry mergers would have to preferentially add material to large radii, realized through many stochastic events spread over a protracted period. We propose that this history is represented by the extended, outer component identified through our photometric decomposition.

We end by briefly comparing our decomposition results with predictions from recent numerical simulations for the formation of massive ETGs. After separating the final stellar system into its in situ (dissipative) and ex situ (accreted) constituents in their simulations, Oser et al. (2010) show that, in comparison to the in situ material, the typical size of the accreted component should correlate with the total stellar mass of the system. Furthermore, the stellar mass fraction of the accreted component may also correlate with the total stellar mass and effective radius of the whole system (Oser et al. 2010; Johansson et al. 2012; Lackner et al. 2012). However, their numerical simulations produce a wide range of possible outcomes: the predictions for the variation of accreted fraction with total stellar mass in Oser et al. (2010) disagree strongly with those from the work of Lackner et al. (2012).

We compare our analysis with the simulations to look for correlations in the accreted components. We assume that the outer and inner+middle components of our multi-component fits approximate the "accreted" and "in situ" material in the theoretical models. Figure 3(a) shows that the effective radius of the outer component of nearby Es does indeed increase strongly with the

total stellar mass of the system, much more so than either of the inner or middle components. While the physical scales and the slope of the correlation are not the same as predicted in the simulations of Oser et al. (2010), there is qualitative agreement. However, the comparison between the accreted fraction, approximated as $M_*^{\rm outer}/M_*^{\rm total}$, and effective radius (Figures 3(b)) and total stellar mass (Figures 3(c)) does not show much, if any, correlation. Apart from the uncertainties of the predictions of current simulations, it is a difficult observational challenge to isolate the accreted component via photometric decomposition. The details of any decomposition are dependent on the choice of specific parameterized model components, which are not unique choices. Also, further galaxy merging would have diluted and partly erased the signatures.

4. SUMMARY AND DISCUSSION

Huang et al. (2013) show that the surface brightness distribution of nearby Es can best be described by three photometrically distinct substructures, consisting of a compact ($R_e \lesssim 1$ kpc) inner component, an intermediate-scale ($R_e \approx 2.5$ kpc) middle component, and an extended ($R_e \approx 10$ kpc) outer envelope. Motivated by the recently proposed two-phase formation scenario for massive galaxies, here we argue that the inner and middle components identified in nearby Es jointly comprise a structure that can be considered the evolved, local counterparts of the high-z compact massive galaxies. In this scenario, these compact structures are derived from highly dissipative processes at high redshifts. Dissipationless minor mergers dominate the late-time evolution of ETGs by contributing to their dramatic size growth. We identify the outer, extended component of nearby Es with this late accretion phase.

Several lines of investigation deserve further attention. In light of the photometric subcomponents uncovered in nearby Es, it is of interest to ask whether such substructure already exists in high-z ETGs, and, if so, whether their gradual buildup can be detected as a function of time. Current studies treat high-z ETGs as single-component systems (e.g., Papovich et al. 2012; Szomoru et al. 2012), but the data may have sufficient quality to allow more complex analysis to reveal potential substructure. Of particular interest is the mechanism by which the "core" structure in massive Es (e.g., Lauer et al. 1995; Kormendy et al. 2009) arises. If scouring by binary supermassive black holes is necessary to make cores (e.g., Hopkins et al. 2009b, 2009c), then major mergers are implicated. Similarly, if high-z massive galaxies contain disky or fast-rotating structures (van der Wel et al. 2011), then they must be destroyed, presumably also through major mergers, if they are to evolve into local massive Es. How do major mergers fit into the framework of the two-phase formation scenario?

Beyond imprints on the photometric structural properties, the two-phase formation scenario also implies differences in stellar population. Recent spectroscopic studies of the faint, outer regions of nearby Es already hint that they have lower metallicity and possibly older age than the inner parts (Coccato et al. 2010; Greene et al. 2012). Photometry is vastly simpler and less expensive than spectroscopy, even if broadband colors provide less robust constraints on stellar populations than spectra. A forthcoming paper will make use of the multi-band CGS data to extract stellar population constraints from the color information of the subcomponents in nearby Es.

We thank the anonymous referee for helpful comments that improved this Letter. We also thank S. Patel for kindly providing us the data from his work. This work was supported by the Carnegie Institution for Science (L.C.H.), the UC Irvine School of Physical Sciences (A.J.B.), the China Scholarship Council (S.H., Z-Y.L.), and the National Natural Science Foundation of China under grants 11133001 and 11273015 (S.H.). S.H. thanks Professor Q.-S. Gu for providing long-term support.

REFERENCES

Bernardi, M., Roche, N., Shankar, F., & Sheth, R. K. 2011, MNRAS, 412, L6
Bezanson, R., van Dokkum, P. G., Tal, T., et al. 2009, ApJ, 697, 1290
Bluck, A. F. L., Conselice, C. J., Buitrago, F., et al. 2012, ApJ, 747, 34
Buitrago, F., Trujillo, I., Conselice, C. J., et al. 2008, ApJL, 687, L61
Cappellari, M., di Serego Alighieri, S., Cimatti, A., et al. 2009, ApJL, 704, L34
Cimatti, A., Nipoti, C., & Cassata, P. 2012, MNRAS, 422, L62
Coccato, L., Gerhard, O., & Arnaboldi, M. 2010, MNRAS, 407, L26
Conselice, C. J., Bluck, A. F. L., Buitrago, F., et al. 2011, MNRAS, 413, 80
Daddi, E., Renzini, A., Pirzkal, N., et al. 2005, ApJ, 626, 680
Damjanov, I., Abraham, R. G., Glazebrook, K., et al. 2011, ApJL, 739, L44
Dekel, A., Sari, R., & Ceverino, D. 2009, ApJ, 703, 785
Fan, L., Lapi, A., De Zotti, G., & Danese, L. 2008, ApJL, 689, L101
Gargiulo, A., Saracco, P., Longhetti, M., La Barbera, F., & Tamburri, S. 2012, MNRAS, 425, 2698
Greene, J. E., Murphy, J. D., Comerford, J. M., Gebhardt, K., & Adams, J. J. 2012, ApJ, 750, 32
Grogin, N. A., Kocevski, D. D., Faber, S. M., et al. 2011, ApJS, 197, 35
Guo, Y., McIntosh, D. H., Mo, H. J., et al. 2009, MNRAS, 398, 1129
Ho, L. C., Li, Z.-Y., Barth, A. J., Seigar, M. S., & Peng, C. Y. 2011, ApJS, 197, 21
Hopkins, P. F., Bundy, K., Murray, N., et al. 2009a, MNRAS, 398, 898
Hopkins, P. F., Cox, T. J., Dutta, S. N., et al. 2009b, ApJS, 181, 135
Hopkins, P. F., Lauer, T. R., Cox, T. J., Hernquist, L., & Kormendy, J. 2009c, ApJS, 181, 486
Huang, S., Ho, L. C., Peng, C. Y., Li, Z.-Y., & Barth, A. J. 2013, ApJ, 766, 47
Johansson, P. H., Naab, T., & Ostriker, J. P. 2012, ApJ, 754, 115
Kormendy, J., Fisher, D. B., Cornell, M. E., & Bender, R. 2009, ApJS, 182, 216
Lackner, C. N., Cen, R., Ostriker, J. P., & Joung, M. R. 2012, MNRAS, 425, 641
Larson, R. B. 1975, MNRAS, 173, 671
Lauer, T. R., Ajhar, E. A., Byun, Y.-I., et al. 1995, AJ, 110, 2622
Li, Z.-Y., Ho, L. C., Barth, A. J., & Peng, C. Y. 2011, ApJS, 197, 22
Negroponte, J., & White, S. D. M. 1983, MNRAS, 205, 1009
Newman, A. B., Ellis, R. S., Bundy, K., & Treu, T. 2012, ApJ, 746, 162
Nipoti, C., Treu, T., Leauthaud, A., et al. 2012, MNRAS, 422, 1714
Onodera, M., Renzini, A., Carollo, M., et al. 2012, ApJ, 755, 26
Oser, L., Ostriker, J. P., Naab, T., Johansson, P. H., & Burkert, A. 2010, ApJ, 725, 2312
Papovich, C., Bassett, R., Lotz, J. M., et al. 2012, ApJ, 750, 93
Patel, S. G., van Dokkum, P. G., Franx, M., et al. 2013, ApJ, 766, 15
Peng, C. Y., Ho, L. C., Impey, C. D., & Rix, H.-W. 2010, AJ, 139, 2097
Prieto, M., Eliche-Moral, M. C., Balcells, M., et al. 2013, MNRAS, 428, 999
Saracco, P., Longhetti, M., & Gargiulo, A. 2011, MNRAS, 412, 2707
Scarlata, C., Carollo, C. M., Lilly, S., et al. 2007, ApJS, 172, 406
Scoville, N., Abraham, R. G., Aussel, H., et al. 2007, ApJS, 172, 38
Sérsic, J. L. 1968, Atlas de Galaxias Australes (Córdoba: Obs. Astron., Univ. Nac. Córdoba)
Szomoru, D., Franx, M., & van Dokkum, P. G. 2012, ApJ, 749, 121
Tasca, L. A. M., Kneib, J.-P., Iovino, A., et al. 2009, A&A, 503, 379
Toomre, A., & Toomre, J. 1972, ApJ, 178, 623
Trujillo, I., Feulner, G., Goranova, Y., et al. 2006, MNRAS, 373, L36
van der Wel, A., Rix, H.-W., Wuyts, S., et al. 2011, ApJ, 730, 38
van Dokkum, P. G., Whitaker, K. E., Brammer, G., et al. 2010, ApJ, 709, 1018